Needleless Vaccine Delivery Using Micro-Shock Waves[▽][†]

Gopalan Jagadeesh,[1]* G. Divya Prakash,[1,2] S. G. Rakesh,[1]‡ Uday Sankar Allam,[2] M. Gopala Krishna,[2] Sandeepa M. Eswarappa,[2]§ and Dipshikha Chakravortty[2]*

Department of Aerospace Engineering, Indian Institute of Science, Bangalore 560012, India,[1] and Department of Microbiology and Cell Biology, Indian Institute of Science, Bangalore 560012, India[2]

Shock waves are one of the most efficient mechanisms of energy dissipation observed in nature. In this study, utilizing the instantaneous mechanical impulse generated behind a micro-shock wave during a controlled explosion, a novel nonintrusive needleless vaccine delivery system has been developed. It is well-known that antigens in the epidermis are efficiently presented by resident Langerhans cells, eliciting the requisite immune response, making them a good target for vaccine delivery. Unfortunately, needle-free devices for epidermal delivery have inherent problems from the perspective of the safety and comfort of the patient. The penetration depth of less than 100 μm in the skin can elicit higher immune response without any pain. Here we show the efficient utilization of our needleless device (that uses micro-shock waves) for vaccination. The production of liquid jet was confirmed by high-speed microscopy, and the penetration in acrylamide gel and mouse skin was observed by confocal microscopy. *Salmonella enterica* serovar Typhimurium vaccine strain pmrG-HM-D (DV-STM-07) was delivered using our device in the murine salmonellosis model, and the effectiveness of the delivery system for vaccination was compared with other routes of vaccination. Vaccination using our device elicits better protection and an IgG response even at a lower vaccine dose (10-fold less) compared to other routes of vaccination. We anticipate that our novel method can be utilized for effective, cheap, and safe vaccination in the near future.

Shock waves appear in nature whenever the different elements in a fluid approach one another with a velocity faster than the local speed of sound (8). Shock waves are essentially nonlinear waves that propagate at supersonic speeds. Such disturbances occur in steady transonic or supersonic flows during explosions, earthquakes, tsunamis, lightning strikes, and contact surfaces in laboratory devices. Any sudden release of energy (within a few microseconds) will invariably result in the formation of a shock wave, since it is one of the efficient mechanisms of energy dissipation observed in nature. The dissipation of mechanical, nuclear, chemical, and electrical energy in a limited space will result in the formation of a shock wave. However, it is possible to generate micro-shock waves in the laboratory by different methods, including controlled explosions. One of the unique features of shock wave propagation in any medium (solid, liquid, or gases) is their ability to instantaneously increase the pressure and temperature of the medium. Researchers are exploiting this behavior of shock waves

to develop novel experimental tools/technologies that transcend the traditional boundaries of basic science and engineering (11). Shock waves have been used successfully for disintegrating kidney stones (16), noninvasive angiogenic therapy (10), and osteoporosis treatment (29). In the present study, we have generated a novel method to produce micro-shock waves using microexplosions. Further utilizing the impulse behind such microblasts, we have developed a novel needleless device for delivering drugs and vaccines into biological systems in a nonintrusive fashion (G. Jagadeesh, 2009, U.S. patent application 12480514).

Drug delivery plays a pivotal role in the field of human health care where nearly 12 billion injections are administered annually for medical purposes, 3% of which are used for immunization (21). Throughout the world, 0.7% of deaths and 0.6% of disability-adjusted life years (DALYs) are caused by contaminated injections in health care settings (17). In low- and middle-income countries, the possibility of HIV transmission through contaminated injections is high (14, 25). Each year, unsafe injections cause an estimated 1.3 million early deaths, loss of 26 million years of life, and an annual burden of $535 million (U.S. dollars) in direct medical expenses. In four out of six parts of the world, more than 30% of the immunization injections are unsafe per the WHO estimation (20). Apart from the unsafe injections, needle injuries, accidental needle sticks, needle phobia, and possible side effects due to transiently high plasma drug concentration are very common (2). A needle-free delivery system that can deliver the drug either actively or passively is a rational alternative. In the case of delivering the drug actively, a driving force is necessary for the transport of drug across the skin, which may be accomplished using jet injectors, electroporation, iontophoresis, ultra-

---

* Corresponding author. Mailing address for Dipshikha Chakravortty: Department of Microbiology and Cell Biology, Indian Institute of Science, Bangalore 560012, India. Phone: 91 80 2293 2842. Fax: 91 80 2360 2697. E-mail: dipa@mcbl.iisc.ernet.in. Mailing address for Gopalan Jagadeesh: Department of Aerospace Engineering, Indian Institute of Science, Bangalore 560012, India. Phone: 91 80 2293 3030. Fax: 91 80 2260 6250. E-mail: jaggie@aero.iisc.ernet.in.

‡ Present address: Department of Mechanical Engineering, Amrita School of Engineering, Amrita Vishwa Vidyapeetham, Bangalore 560035, India.

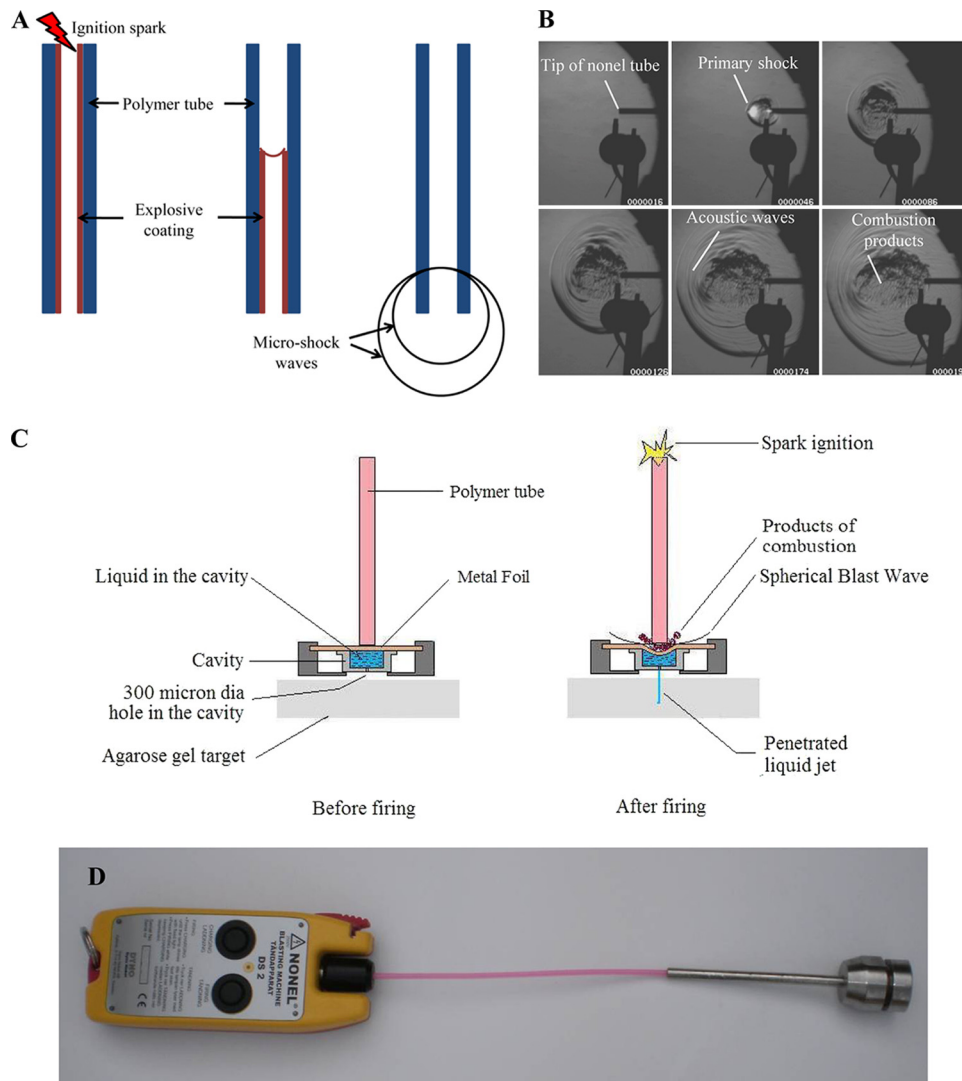§ Present address: Lerner Research Institute, Cleveland Clinic, Cleveland, OH 44195.

FIG. 1. (A) Schematic diagram of micro-shock wave generation from the polymer tube shows the initiation of ignition of the polymer tube by a spark generated by electrodes, the explosive coating undergoing combustion, the combustion flame front traveling at 2,000 m/s, and the micro-shock wave emanating from the open end of the polymer tube. (B) Sequential schlieren images of the micro-shock wave propagation from the open-end polymer tube. (C) Diagram showing pictorial views of the fluid jet delivery system before and after firing. dia, diameter. (D) Prototype model of the needleless delivery device.

sound, powder injection, and tape stripping (2). Different delivery systems have been developed to deliver vaccine to the epidermal layer of skin (4, 28). Recently, a novel polymer-based microneedle technology has been developed for vaccination (28), and the existing microneedle technology has also been checked for intradermal delivery of vaccine (1, 27). However, the available needleless delivery systems have their own limitations, such as cost, cross contamination, pain, and bleeding (21). In this study, we have demonstrated efficient vaccination in a murine model using our novel needleless device.

MATERIALS AND METHODS

Development of a needle-free delivery device. A simple and novel methodology to generate micro-blast waves in a repeatable fashion and in a controlled manner using a small amount of explosives was developed. A simple prototype model was developed to transfer the energy of micro-blast waves to the liquid. The delivery device consists of an ignition system, a polymer tube coated with explosive material, metal foil, drug-holding chamber, and cavity holder (Fig. 1D).

Time-resolved schlieren technique. A high-speed digital camera, Phantom 7.1 (Vision Research Inc.), that is capable of recording 6,688 frames per second at a resolution of 800 by 600 pixels using a self-resetting complementary metal oxide semiconductor (SR-CMOS) imaging array is used for this experiment. The schlieren images were recorded by operating the camera at a speed of 10,000 frames per second with a resolution of 450 by 450 pixels and an exposure time of 3 μs. A 300-W, continuous halogen light source is used in these experiments, and the operation of the camera is synchronized with the polymer tube firing operation using a trigger pulse generated by the pressure sensor located at the open end of the polymer tube.

Pressure measurement experiment. The pressure acting on the liquid inside the cavity was found using a polyvinyl difluoride (PVDF)-coated needle hydrophone (Dr. Müller Instruments, Oberursel, Germany). The needle gauge is inserted into the cavity at a distance of 3 mm from the foil surface (i.e., at the mouth of the 300-μm hole). The cavity was completely filled with the liquid (water), and metal foil was placed on top of the cavity. This arrangement was kept inside the device, and the metal foil was subjected to the micro-shock wave loading by igniting the explosive material inside the polymer tube. The pressure

signals picked up by the needle gauge are recorded by the oscilloscope (Yokogawa Electric Corporation, Japan).

Bacterial strains used in this study. Bacterial strains used in this study are described in Table S1 in the supplemental material.

Effect of micro-shock waves on the viability of bacteria. Gram-negative (*Salmonella enterica* and *Escherichia coli*) and Gram-positive (*Listeria monocytogenes*) bacteria were used as models to study the effect of micro-shock waves on the bacteria. Cultures grown overnight were centrifuged, and the pellets were resuspended in sterile phosphate-buffered saline (PBS). The resuspended culture was loaded in the device, and after the explosion, the bacteria were delivered to the microcentrifuge tube. The cultures were serially diluted and plated on Salmonella-Shigella (SS) agar, LB agar, and brain heart infusion (BHI) medium for *S. enterica*, *E. coli*, and *L. monocytogenes*, respectively. An equal volume of untreated culture was plated as a control.

Delivery of bacteria using the device. BALB/c mice were bred and housed at the Central Animal Facility at the Indian Institute of Science. The mice used for the experiments were 6 to 8 weeks old. All procedures with animals were carried out in accordance with the institution rules for animals. Hair on the skin was removed in the abdomen region using a hair clipper or commercial hair removal cream before the delivery of *S. enterica* serovar Typhimurium vaccine strain pmrG-HM-D (DV-STM-07) using the device. The delivery device was placed in a perpendicular position against the shaved abdominal skin of the mice, and the delivery of vaccine was carried out.

DV-STM-07 was administered to mice orally (10^7 CFU/mouse), intraperitoneally (i.p.) (10^4 CFU/mouse), and using the device (10^3 CFU/mouse) (5 mice in each group). DV-STM-07 was applied for 2 min to the skin of the appropriate controls (mice with hair removed) and then wiped using 70% ethanol to check the effect of hair removal. Mice were not fed for 12 h before oral infection. The mice were sacrificed after 3 days, and the liver, spleen, and mesenteric lymph nodes (MLN) were aseptically isolated, weighed, and homogenized in sterile PBS. The homogenate was plated in serial dilutions on SS agar to determine the bacterial load in various organs. The number of CFU was counted and shown as CFU/gram of organ.

Confocal microscopy. Penetration of liquid jet into the polyacrylamide gel and skin of mice was confirmed using confocal laser scanning microscopy (LSM meta; Zeiss). Carboxylate-modified polystyrene fluorescent yellow-green latex beads (catalog no. L4655; Sigma-Aldrich) (4.6×10^9 particles per ml) and *Salmonella* Typhimurium expressing green fluorescent protein (GFP) were administered to mice using the device as described above. The skin was removed and mounted on a glass slide and immediately visualized using a confocal microscope. Images were obtained in *xyz* scanning mode and captured every 2 μm from the skin surface until no appreciable fluorescence could be detected.

Biofluorescence imaging. Fluorescent yellow-green latex beads (catalog no. L4655; Sigma-Aldrich) with a size of 1 μm were taken at a concentration of 4.6×10^9 particles per ml and delivered to the dorsal side of mice using the device as mentioned above. The excitation passband (445 to 490 nm) and emission passband (515 to 575 nm) were set for GFP. Immediately after the delivery of fluorescent beads, mice were anesthetized with gaseous 5% isoflurane in O_2 and imaged using a Xenogen IVIS 200 imaging system. The animals were placed in a ventral recumbent position and imaged from the dorsal aspect.

Immunization of mice. DV-STM-07 was used as the vaccine strain in this study. The mice (6 mice per group) were immunized (10^3 CFU/mouse) using the device as described above with proper controls. PBS was given to mice by using the device as a control. Positive-control mice were vaccinated intraperitoneally (10^4 CFU/mouse). After 5 days, all mice were challenged orally with virulent *Salmonella* for organ burden (10^7 CFU/mouse) and for survival assay (10^8 CFU/mouse). Mice were observed twice a day for morbidity and mortality.

Estimation of serum immunoglobulin G (IgG). Blood samples were collected from the ocular vein of each mouse. Serum samples were collected by centrifugation and stored at $-80°C$ until use. All serum samples were diluted in PBS supplemented with 1% bovine serum albumin (BSA) prior to use in an enzyme-linked immunosorbent assay (ELISA). ELISA was performed as mentioned elsewhere with some modifications (5).

The serum IgG titer specifically for *Salmonella* lipopolysaccharide (LPS) was measured by an ELISA. LPS (250 ng/100 μl/well) in 0.02% trichloroacetic acid was used to coat the wells in the ELISA plate. The plates were incubated at 37°C for 2 h, and the wells were subsequently blocked for 1 h at room temperature with 3% BSA. One hundred microliters of diluted serum was added to each well, the plate was incubated for 1 h at 37°C, and the wells were washed. Horseradish peroxidase (HRP)-conjugated anti-IgG antibody (1:10,000 dilutions) was added to the wells, and the plate was incubated for 1 h at 37°C. After the wells were washed, 100 μl of tetramethylbenzidine solution was added to each well and incubated for 15 min. Fifty microliters of 1 N H_2SO_4 was added to stop the reaction, and the optical density (OD) was measured at 450 nm. The highest dilution at which the absorbance of the sample exceeds the background absorbance by 2 standard deviations was taken as the endpoint titer of the sera.

Statistical analysis. The data were subjected to statistical analysis by applying Student's *t* test and Mann-Whitney U test using Graph Pad Prism 5 software, and a *P* value of <0.05 was considered significant. The mortality and survival data were analyzed using the log rank test. All the experiments were repeated at least three times to confirm the results.

RESULTS AND DISCUSSION

In the present study, the instantaneous release of a finite amount of chemical energy is used for generating controlled micro-shock waves in the laboratory. The method uses small amounts (~18 mg/m) of explosive (high melting explosive [octahydro-1,3,5,7-tetranitro-1,3,5,7-tetrazocine] and traces of aluminum) uniformly coated on the inner wall of a polymer tube of arbitrary length. When the microexplosive is ignited from one end of the polymer tube, a detonation wave is generated inside the tube, and the products of microexplosion are allowed to emanate from the open end. The release of a finite amount of energy (equivalent to 0.168 mg of trinitrotoluene) from the open end of polymer tube invariably generates spherical micro-shock waves (Fig. 1A). The sequential images of micro-shock waves emanating from the open end of the polymer tube were captured by a time-resolved schlieren technique (15) using a high-speed camera (Fig. 1B; see the video in the supplemental material).

After the microexplosion, instead of allowing the energy to be dissipated in the open, a thin metal foil is used to transfer the impulse momentum to the liquid, which is in a cylindrical drug-holding chamber (Fig. 1C). A 300-μm-diameter hole at the bottom of this chamber in the absence of an external force acts like a valve owing to the surface tension of the liquid and does not allow the drug to exit the chamber. The polymer tube is positioned in the top of the chamber and just touches the surface of a thin (100-μm-thick) brass foil. When the metal foil is exposed to a high-pressure impulse, it deflects instantaneously, transferring all the momentum to the liquid underneath, thereby causing instantaneous compression of the liquid column, which drives the liquid through the discharge hole as a liquid jet. On the basis of this phenomenon, a novel needleless vaccine delivery device was developed (Fig. 1D). Enough safety precautions by way of miniature rubber gaskets have been incorporated in the device to ensure that the gaseous products of combustion do not leak through the drug-holding chamber. The velocity of the jet coming out of the discharge hole depends on the instantaneous pressure acting on the liquid column inside the cavity. The maximum pressure observed by the liquid inside the cavity was more than 6.0×10^6 Pa (Fig. 2A). High-speed flow visualization studies have shown that the liquid jet comes out at a very high velocity (>100 m/s) from the chamber and penetrates into the target material. This energy transfer mechanism was used to deliver the liquid jet and was tested in 4% agarose gels and 20% polyacrylamide gels (skin model [26]) for the penetration studies (Fig. 2B and C). In a 4% agarose gel, the penetration depth of the water was about 2 mm, whereas in a 20% polyacrylamide gel, the penetration depth of the fluorescent latex bead mix was about 60 μm. Initially, an agarose gel was used to check the penetration of the liquid jet. The polyacrylamide gel consist of a cross-
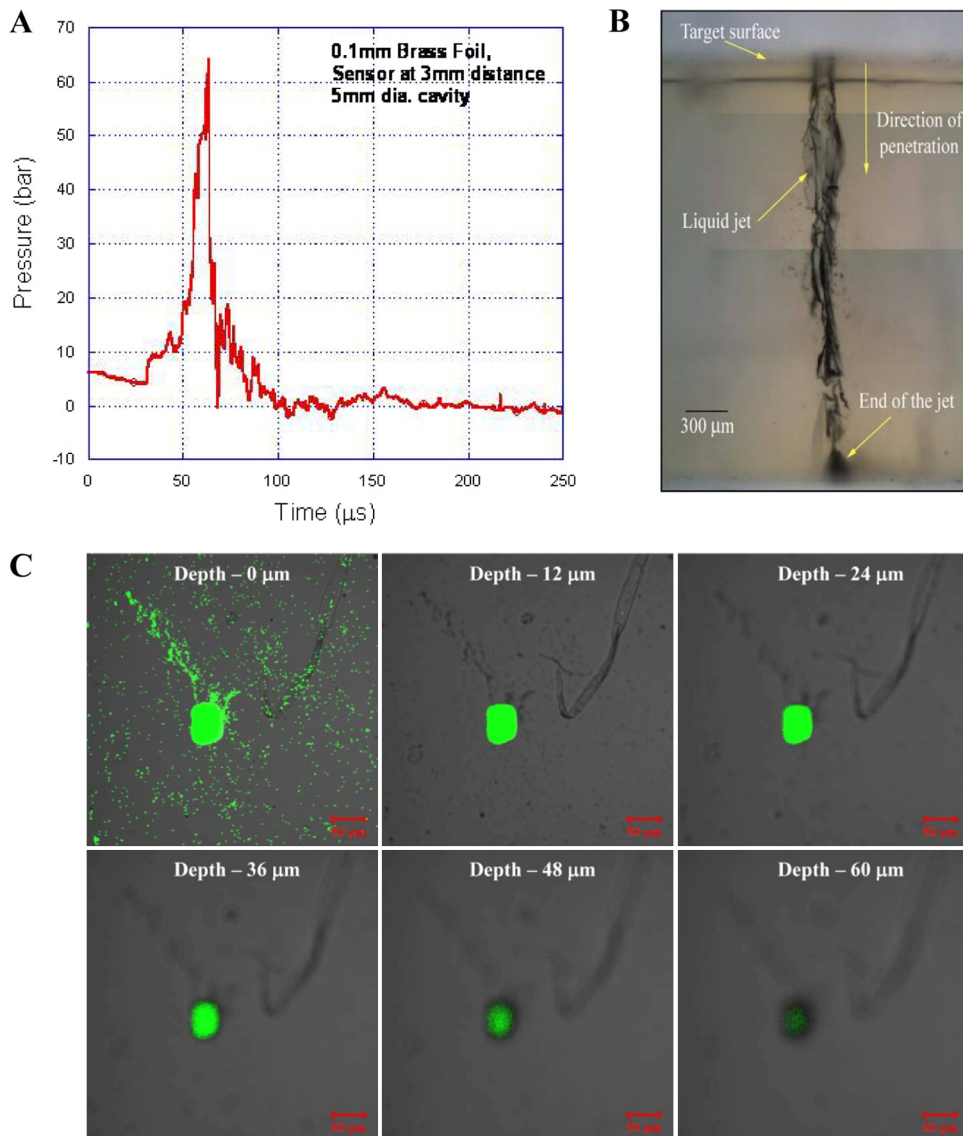
FIG. 2. Liquid jet delivery from the device. (A) Graph showing variation in pressure in the liquid inside the chamber of the device over time. (1 bar = 10^5 Pa). (B) Microscopic image of liquid (water) jet delivered into the 4% agarose gel target merged using Adobe Photoshop. (C) Confocal images showing the penetration of fluorescent yellow-green latex beads delivered to 20% acrylamide gels using the device.

linked polymer with a high tensile strength (26) and small pore size, whereas the agarose gel has a larger pore size and comparably less tensile strength (24). The penetration depth was higher in the agarose gel because of the mechanical properties of the gel. The polyacrylamide gel, which is being used as a skin model because of the matrix structure of the polymer and mechanical property (26), was used to check the efficiency of the device before starting *in vivo* studies.

Before using the needleless delivery device for vaccine delivery, it was necessary to check the effect of shock waves on the vaccine strain, since earlier studies have documented deleterious effects on bacteria (7) and rat brain (12) upon exposure to shock waves. *Salmonella enterica* serovar Typhimurium vaccine strain pmrG-HM-D (DV-STM-07), *Escherichia coli* (Gram-negative), and *Listeria monocytogenes* (Gram-positive) bacteria were used to test the effect of micro-

shock waves. The pressure waves produced by the device for ultrashort duration (microseconds) had no effect on the viability of both Gram-negative and Gram-positive bacteria (Fig. 3A). The effectiveness of DV-STM-07 (D. Chakravortty and V. D. Negi, 22 August 2008, international patent application PCT/IN2008/000524) as a vaccine has been demonstrated previously (22, 23) and was used as the vaccine strain in our study. The delivery device was tested for its efficacy of vaccination in the mouse model. There were no macroscopically visible injuries like bleeding, edema, or any other local reactions at the site of vaccination on the skin, immediately after delivery and up to 10 days after vaccination. DV-STM-07 given through the device (10^3 CFU/mouse) reached the secondary lymphoid organs (spleen, liver, and mesenteric lymph nodes [MLN]) at levels comparable to those of other modes of vaccine delivery (Fig. 3B).

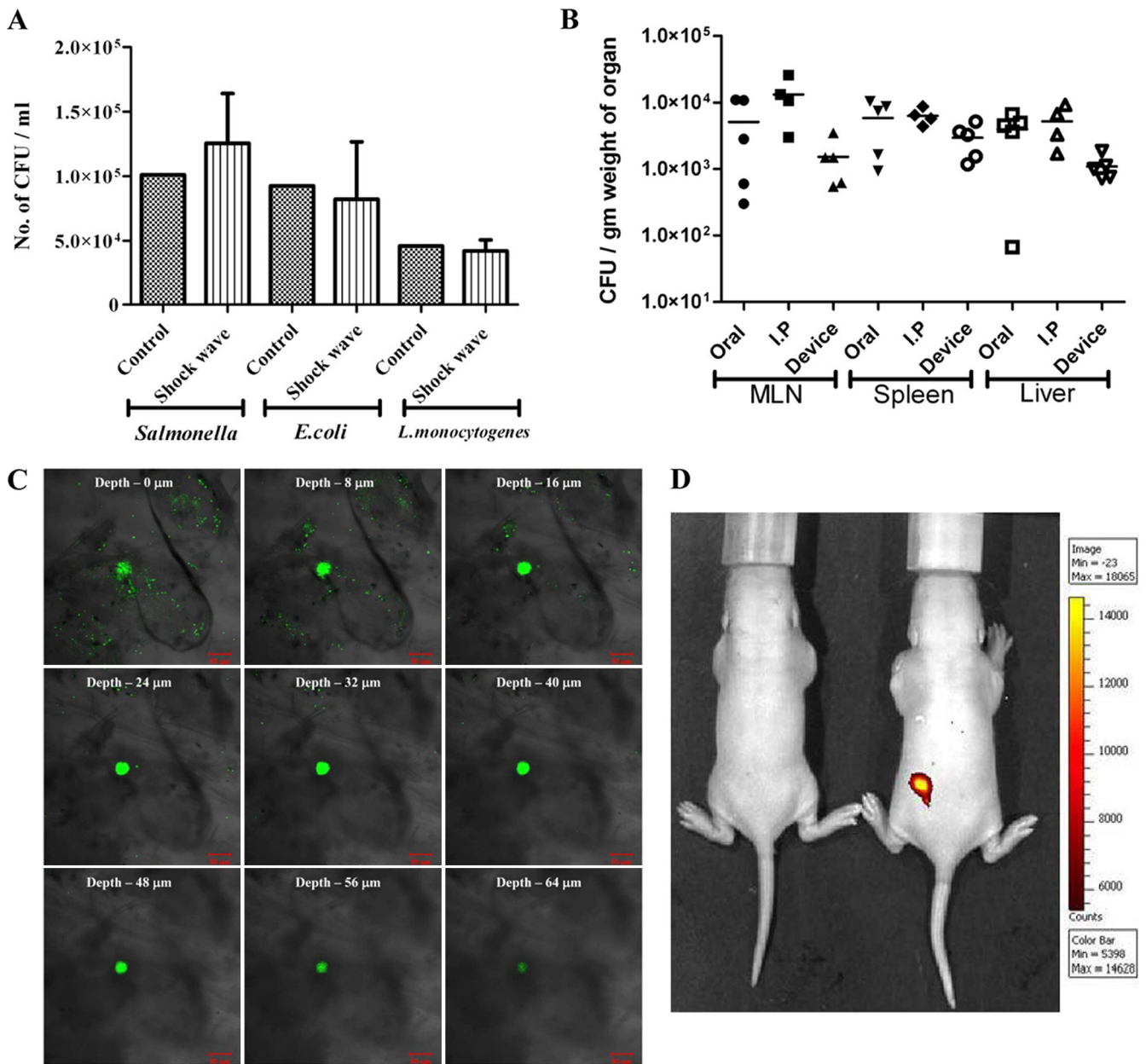Fluorescent yellow-green latex beads of ~1 µm in size were

FIG. 3. *In vitro* and *in vivo* testing of the device. (A) Gram-negative (*Salmonella* and *E. coli*) and Gram-positive (*Listeria*) bacterial cultures were placed in the cavity (without a discharge hole) and subjected to micro-shock waves to check the viability of bacteria using the device. The control bacterial culture was not subjected to micro-shock wave treatment. (B) *Salmonella enterica* serovar Typhimurium vaccine strain pmrG-HM-D (DV-STM-07) was administered to mice using the device, and the mice were sacrificed and dissected after 3 days to check the entry of bacteria in secondary lymphoid organs like mesenteric lymph nodes (MLN), spleen, and liver. In the control mice, DV-STM-07 was delivered by the oral or intraperitoneal (I.P) route. Each symbol represents the value for an individual mouse. The short black line shows the mean value for the group (5 mice in each group). (C) Confocal images (*xyz* scanning) showing the penetration of fluorescent beads delivered to the abdominal region of mouse skin using the device. (D) Fluorescent beads were delivered to the dorsal side of mice using the device, and a biofluorescence image showing the presence of fluorescent beads is shown. Min, minimum; Max, maximum.

used as a model for bacteria and were delivered to the abdominal region of the mouse using the device. The presence of fluorescent beads in the skin was confirmed by confocal microscopy. The fluorescent beads (Fig. 3C) and *Salmonella* expressing green fluorescent protein (see Fig. S1 in the supplemental material) were found to penetrate the skin to a depth of up to 50 to 80 μm. This shows that the device can deliver the vaccine effectively into the epidermis and dermis region of the skin. Biofluorescence imaging was also carried out to confirm the presence of fluorescent beads in the mouse model (Fig. 3D). The overall results show that the device can be used for effective vaccine delivery. DV-STM-07 delivered with this device does not penetrate deeper than the skin but may be localized in the epidermis and dermis layer of the skin (3).
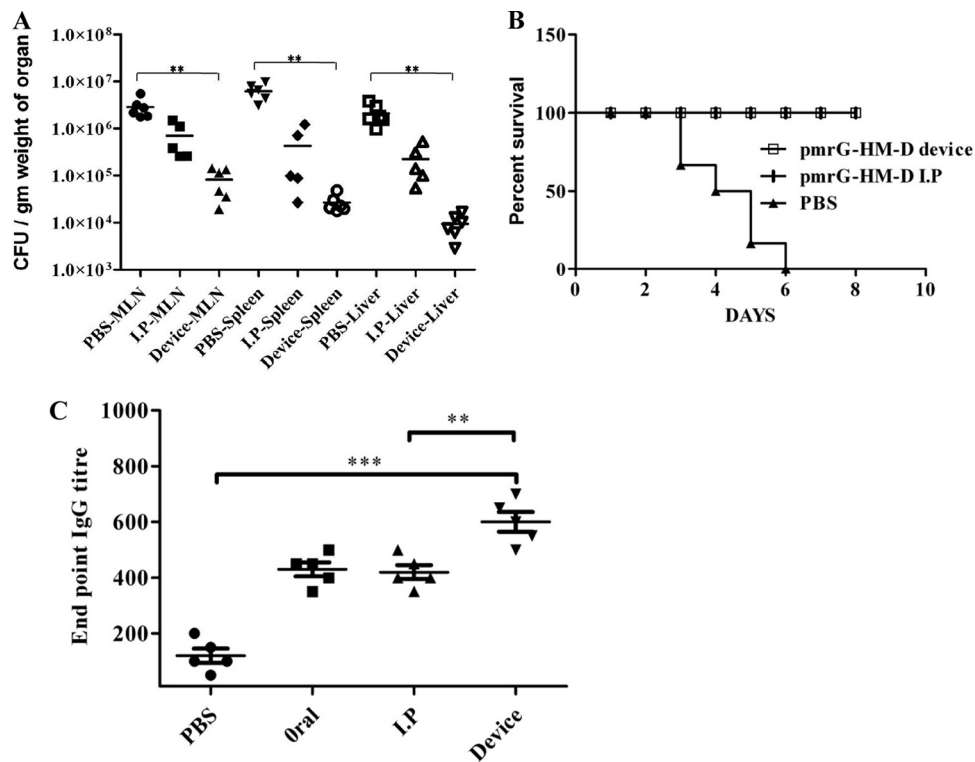
FIG. 4. Efficiency of vaccine delivery using the device. (A) *S. enterica* serovar Typhimurium vaccine strain pmrG-HM-D (DV-STM-07) was administered to mice using the device and by the intraperitoneal (I.P) route. The control mice were given phosphate-buffered saline (PBS) delivered using the device. Mice were infected with a lethal dose (10^7 CFU/mouse) of virulent *Salmonella* orally, 5 days after the immunization. The MLN, spleen, and liver were aseptically dissected to check the *Salmonella* burden 4 days after the challenge. Values that are statistically significantly different ($P < 0.005$ by the Mann-Whitney U test) are indicated by the bracket and two asterisks. (B) Mice (6 mice per group) were infected with a lethal dose (10^8 CFU/mouse) of virulent *Salmonella* orally 5 days after immunization as described for the previous experiment, and the percent survival of mice over time was determined. The values for the vaccinated mice and the control mice that were treated with PBS were significantly different ($P < 0.0001$ by the log rank test). (C) A single dose of DV-STM-07 was delivered using the device, orally, and by the intraperitoneal route, and the serum IgG levels were tested against *Salmonella*-specific lipopolysaccharide (LPS) using ELISA. Control mice were given PBS delivered using the device. Each symbol represents the value for an individual mouse. The mean value (black line) ± standard deviation (error bars) for each group of mice are shown. Values that are significantly different by Student's *t* test are indicated by the bracket and asterisks as follows: **, $P < 0.005$; ***, $P < 0.0005$.

In order to determine the efficiency of our device in delivering the vaccine, we immunized the mice with DV-STM-07 (10^3 CFU/mouse) using the device and then challenged the mice with virulent *Salmonella* (10^7 CFU/mouse) orally after 5 days. Mice immunized by the intraperitoneal (i.p.) route (10^4 CFU/mouse) were used as a positive control, and the *Salmonella* burden in the secondary lymphoid organs (MLN, spleen, and liver) was evaluated 4 days after the challenge. In the immunized mice, there was a minimum of 100-fold reduction in the *Salmonella* load in the organ compared to the organs of placebo control mice ($P < 0.0007$) (Fig. 4A). Surprisingly, it was observed that mice vaccinated by using the device had a lower organ burden than the mice immunized i.p. Vaccination using our device showed better efficiency even with 10% of the dose given to the controls. In the survival assay, mice vaccinated using the device and mice vaccinated i.p. showed 100% survival upon challenge with virulent *Salmonella* (10^8 CFU/ mouse), whereas all the unvaccinated mice died within 8 days after the challenge ($P < 0.0001$) (Fig. 4B). Additional controls were used to check the effect of hair removal in mice before vaccination. DV-STM-07 (10^4 CFU/mouse) was applied to

skin after the removal of hair using a hair clipper or commercial hair removal cream. After challenge with virulent *Salmonella*, the bacterial burdens in different organs were assessed. These mice showed no significant difference from the mice in the control group in organ load and in the survival assay (data not shown). These results clearly demonstrate that vaccination using the new micro-shock wave-assisted device measures up to the traditional vaccination strategies in this efficacy of protection even at the reduced dose. Even though there is a significant difference in the bacterial loads of the group vaccinated by the i.p. route and the group vaccinated using the device in Fig. 4A, there is no difference in morbidity or body weight.

We measured antibody responses in serum samples using an enzyme-linked immunosorbent assay (ELISA). After a single immunization of mice with DV-STM-07 using the device (10^3 CFU/mouse), the serum immunoglobulin G (IgG) titer specific to *Salmonella* lipopolysaccharide (LPS) was measured after 5 days. The IgG endpoint titer was significantly higher than when the vaccine was given by the oral or i.p. route ($P < 0.0033$) (Fig. 4C). This shows that the reduced dose that can be given with our device can induce a significantly higher humoral re-

sponse. This may due to the efficient antigen-presenting Langerhans cells present in the epidermal layer of the skin.

The delivery of vaccine at a penetration depth of less than 100 μm may not elicit pain (13, 18). The mice did not make a sound during vaccine administration with the device, whereas they made sounds during needle injections. This shows that the device can deliver vaccine in the epidermal layer of skin where there are no sensitive pain nerve endings. Therefore, vaccine administration using the device will not elicit any acute pain in mice.

Studies show that intradermal vaccination offers better protection than the other routes of immunization (9). The delivery of vaccines to the epidermal layer of the skin is a major challenge while using needle injections. Administering vaccine to the epidermal layer of skin can be done with high efficiency using our device. Delivering vaccines in close proximity to the epidermal layer may facilitate the antigen recognition and uptake process by Langerhans cells (19). Since intradermal injection of hepatitis B and rabies vaccines required only 10% of an intramuscular dose to elicit an equivalent antibody response and seroconversion rate (6), the dose of vaccine can be reduced by using our device. The cost of our needleless device will be $200, and the cost per shot will be 10 cents. As sensitive nerve endings are not present in the epidermal layer of skin, delivery of vaccine using our device will be safer than intradermal needle injection. Given that most of the vaccines commercially available are in liquid formulations, our device can be used to deliver those vaccines regardless of their particle size and chemical nature. Its potential use to deliver insulin has far-reaching consequences, because diabetics have to take insulin at least twice a day for the rest of their lives. For them, this device will be a welcome relief. Optimizing the size of the liquid drug-holding chamber to different doses, changing the size of the discharge hole as a function of the viscosity of the liquid drug, and exploring the possibility of integrating the present device with an endoscopic catheter are some of the issues that will be addressed in future studies.

REFERENCES

1. **Alarcon, J. B., A. W. Hartley, N. G. Harvey, and J. A. Mikszta.** 2007. Preclinical evaluation of microneedle technology for intradermal delivery of influenza vaccines. Clin. Vaccine Immunol. **14:**375–381.
2. **Arora, A., M. R. Prausnitz, and S. Mitragotri.** 2008. Micro-scale devices for transdermal drug delivery. Int. J. Pharm. **364:**227–236.
3. **Azzi, L., M. El-Alfy, C. Martel, and F. Labrie.** 2005. Gender differences in mouse skin morphology and specific effects of sex steroids and dehydroepiandrosterone. J. Investig. Dermatol. **124:**22–27.
4. **Chen, D., et al.** 2000. Epidermal immunization by a needle-free powder delivery technology: immunogenicity of influenza vaccine and protection in mice. Nat. Med. **6:**1187–1190.
5. **Chen, D., et al.** 1996. Evaluation of purified UspA from Moraxella catarrhalis as a vaccine in a murine model after active immunization. Infect. Immun. **64:**1900–1905.
6. **Fadda, G., et al.** 1987. Efficacy of hepatitis B immunization with reduced intradermal doses. Eur. J. Epidemiol. **3:**176–180.
7. **Gerdesmeyer, L., et al.** 2005. Antibacterial effects of extracorporeal shock waves. Ultrasound Med. Biol. **31:**115–119.
8. **Griffith, W. C.** 1981. Shock waves. J. Fluid Mechanics **106:**81–101.
9. **Hunsaker, B. D., and L. J. Perino.** 2001. Efficacy of intradermal vaccination. Vet. Immunol. Immunopathol. **79:**1–13.
10. **Ito, K., Y. Fukumoto, and H. Shimokawa.** 2009. Extracorporeal shock wave therapy as a new and non-invasive angiogenic strategy. Tohoku J. Exp. Med. **219:**1–9.
11. **Jagadeesh, G.** 2008. Industrial applications of shock waves. Proc. Inst. Mech. Eng. Part G. J. Aerospace Eng. **222:**575–583.
12. **Kato, K., et al.** 2007. Pressure-dependent effect of shock waves on rat brain: induction of neuronal apoptosis mediated by a caspase-dependent pathway. J. Neurosurg. **106:**667–676.
13. **Kaushik, S., et al.** 2001. Lack of pain associated with microfabricated microneedles. Anesth. Analg. **92:**502–504.
14. **Kermode, M.** 2004. Unsafe injections in low-income country health settings: need for injection safety promotion to prevent the spread of blood-borne viruses. Health Promot. Int. **19:**95–103.
15. **Kleine, H., et al.** 2005. High-speed time-resolved color schlieren visualization of shock wave phenomena. Shock Waves **14:**333–341.
16. **Lingeman, J. E., J. A. McAteer, E. Gnessin, and A. P. Evan.** 2009. Shock wave lithotripsy: advances in technology and technique. Nat. Rev. Urol. **6:**660–670.
17. **Lopez, A. D., C. D. Mathers, M. Ezzati, D. T. Jamison, and C. J. L. Murray (ed.).** 2006. Global burden of disease and risk factors. The World Bank, Washington, DC.
18. **McAllister, D. V., et al.** 2003. Microfabricated needles for transdermal delivery of macromolecules and nanoparticles: fabrication methods and transport studies. Proc. Natl. Acad. Sci. U. S. A. **100:**13755–13760.
19. **Merad, M., F. Ginhoux, and M. Collin.** 2008. Origin, homeostasis and function of Langerhans cells and other langerin-expressing dendritic cells. Nat. Rev. Immunol. **8:**935–947.
20. **Miller, M. A., and E. Pisani.** 1999. The cost of unsafe injections. Bull. World Health Organ. **77:**808–811.
21. **Mitragotri, S.** 2005. Immunization without needles. Nat. Rev. Immunol. **5:**905–916.
22. **Negi, V. D., A. G. Nagarajan, and D. Chakravortty.** 2010. A safe vaccine (DV-STM-07) against Salmonella infection prevents abortion and confers protective immunity to the pregnant and new born mice. PLoS One **5:**e9139.
23. **Negi, V. D., S. Singhamahapatra, and D. Chakravortty.** 2007. Salmonella enterica serovar Typhimurium strain lacking pmrG-HM-D provides excellent protection against salmonellosis in murine typhoid model. Vaccine **25:**5315–5323.
24. **Normand, V., D. L. Lootens, E. Amici, K. P. Plucknett, and P. Aymard.** 2000. New insight into agarose gel mechanical properties. Biomacromolecules **1:**730–738.
25. **Reid, S.** 2009. Increase in clinical prevalence of AIDS implies increase in unsafe medical injections. Int. J. STD AIDS **20:**295–299.
26. **Schramm-Baxter, J., J. Katrencik, and S. Mitragotri.** 2004. Jet injection into polyacrylamide gels: investigation of jet injection mechanics. J. Biomech. **37:**1181–1188.
27. **Song, J. M., et al.** 2010. Microneedle delivery of H5N1 influenza virus-like particles to the skin induces long-lasting B- and T-cell responses in mice. Clin. Vaccine Immunol. **17:**1381–1389.
28. **Sullivan, S. P., et al.** 2010. Dissolving polymer microneedle patches for influenza vaccination. Nat. Med. **16:**915–920.
29. **van der Jagt, O. P., et al.** 2009. Unfocused extracorporeal shock wave therapy as potential treatment for osteoporosis. J. Orthop. Res. **27:**1528–1533.